https://doi.org/10.5194/egusphere-2025-4292
Preprint. Discussion started: 23 September 2025

Recent intensification of extreme precipitation over Antarctica driven by increases in greenhouse gases

Sai Prabala Swetha Chittella[1,2], Andrew Orr[2], Pranab Deb[1], and Quentin Dalaiden[3]

[1]Centre for Ocean, River, Atmosphere and Land Sciences (CORAL), Indian Institute of Technology Khargapur, Khargapur, 721302, India

[2]British Antarctic Survey, National Environmental Research Council, Cambridge, UK

[3]Nansen Environmental and Remote Sensing Center and Bjerknes Center for Climate Research, Bergen, Norway

Correspondence to: Sai Prabala Swetha Chittella (prabala.saiswetha@gmail.com)

Abstract. Extreme precipitation is a major contributor to the total precipitation over Antarctica, as well as its variability. However, it's still poorly understood whether any recent trends in extreme precipitation over Antarctica have occurred, and if so, whether they are anthropogenically driven. Here we address this knowledge gap by using ERA5 data from 1979 to 2023 to identify six Antarctic drainage basins with significant positive trends in total and extreme precipitation. These basins include one in the Antarctic Peninsula, one in West Antarctica, and four in East Antarctica. We show that these trends are partly due to an increased occurrence of atmospheric rivers. We subsequently perform a detection and attribution analysis of these trends using precipitation outputs from global climate model CESM2 ensembles that consider all external forcing (ALL), greenhouse gases only (GHG), and anthropogenic aerosols only (AAER). Five of the basins (one in West Antarctica and four in East Antarctica) have good agreement between the trends from the ALL ensemble and ERA5, as well as between the ALL and GHG ensembles, indicating that greenhouse gases are the primary driver of the present-day trends in total and extreme precipitation over these basins. The good agreement between the ALL ensemble and ERA5 trends is confirmed using a regression-based detection and attribution technique. However, regressing the ALL, GHG, and AAER ensembles against ERA5 did not yield robust attribution to any specific single-forcing for either total or extreme precipitation, which is likely due to limitations such as the relatively small ensemble size of the simulations.

1 Introduction

Extreme precipitation events (EPEs, i.e., where the amount of precipitation at a location is substantially greater than normal) have increased in intensity and frequency globally in recent decades (Donat et al., 2013; Sun et al., 2020; Dunn et al., 2020; Li et al., 2024), which has been attributed to anthropogenically-induced climate change (Min et al., 2011; Zhang et al., 2013; Paik et al., 2020; Young et al., 2020; Dong et al., 2020, 2021; Seneviratne et al., 2021; Estrada et al., 2023; IPCC 2023). In Antarctica, EPEs account for over 40% of the continent's total precipitation and almost 70% of the variance in annual

https://doi.org/10.5194/egusphere-2025-4292
Preprint. Discussion started: 23 September 2025

precipitation, and are often associated with intense atmosphere rivers (ARs) (Gorodetskaya et al., 2014; Turner et al., 2019; Adusumilli et al., 2021; Wille et al., 2021, 2024a, 2025; Gehring et al., 2022; Maclennan et al., 2022, 2023; Simon et al., 2024). However, identifying positive trends in EPEs over recent decades in Antarctica is hampered by such events being rare and difficult to separate from the substantial interannual precipitation variability that characterises its climate (Connolley, 1997; Hosking et al., 2013; Yu et al., 2018, 2025). Nevertheless, positive trends in the number of EPEs occurring over recent decades have been identified over parts of East Antarctica (Yu et al., 2018; Simon et al., 2024).

Antarctic precipitation and EPEs are the major component of surface mass balance (SMB), and thus play a crucial role in controlling the stability of the Antarctic ice sheet by offsetting dynamically driven ice-losses (Favier et al., 2017; Zwally et al., 2017; Paolo et al., 2018; Rignot et al., 2019; Kittel et al., 2021; Mottram et al., 2021; Davison et al., 2023; Kromer and Trusel, 2023; Otosaka et al., 2023; Wang et al., 2025). Furthermore, mass gained from precipitation and EPEs over Antarctic ice shelves can partially compensate for mass-losses caused by either basal or surface melting (Bintanja et al., 2013; Trusel et al., 2013; Paolo et al., 2015; Nicolas et al., 2017; Pattyn et al., 2017; Gardner et al., 2018; Kuipers Munneke et al., 2018; Rignot et al., 2019; Nakayama et al., 2021; Wille et al., 2022; Johnson et al., 2022; van Wessem et al., 2023). This is especially critical as ice shelf thinning results in the acceleration of grounded ice toward the ocean, where the ice subsequently calves into the ocean as icebergs and causes increased sea-level rise (Rott et al. 1996; Pritchard et al. 2012; Rignot et al. 2019). Additionally, snowfall is an essential factor in minimizing the susceptibility of ice shelves to surface melt pond formation, which can initiate hydrofracturing of ice shelves, by counteracting any firn air depletion caused by surface melting (Scambos et al. 2000; Munneke et al., 2014; Banwell and MacAyeal 2015; Lai et al. 2020; Orr et al., 2023; Van Wessem et al., 2023).

Therefore, a better physical understanding of the trends in EPEs during the past decades over Antarctica is critical. Moreover, an enhanced understanding of the drivers of these trends, such as anthropogenically-induced changes (i.e., external climate forcing), is also of critical importance to better highlight how EPEs and associated impacts might change under future climate projections (Kittel et al., 2021; Vignon et al., 2021). For example, Dalaiden et al. (2022) identified that increased greenhouse gas emissions and stratospheric ozone depletion were the primary drivers of increased precipitation and temperature over West Antarctica since the middle of the twentieth century. These two drivers were also identified as causing recent changes in Southern Ocean temperature and salinity by Swart et al. (2018) and Hobbs et al. (2020). Additionally, increased anthropogenic aerosol emissions in Asia in recent decades have been suggested by Gu et al. (2025) to affect Antarctica's climate by Rossby-wave teleconnections. However, the strong internal variability prevailing in the Southern Hemisphere high latitudes makes the analysis of the forced signal from the observed changes during the past decades highly challenging (e.g., Fyke et al., 2017). For example, the contribution of internal variability to driving changes in sea ice extent is critical and may become even more prominent by the middle of the twenty-first century, potentially reducing the influence of anthropogenically-induced changes on Antarctic precipitation / SMB (Previdi and Polvani, 2016; Morioka et al., 2024).

https://doi.org/10.5194/egusphere-2025-4292
Preprint. Discussion started: 23 September 2025

Nevertheless, although some studies have investigated the drivers of trends of extreme temperatures over Antarctica (e.g., Blanchard-Wrigglesworth et al., 2023; Wille et al., 2024b), our understanding of the drivers of changes in EPEs over Antarctica is still lacking. In this study we therefore perform a detection and attribution (D&A) analysis to investigate the influence of external forcings and natural variability on annual trends in total and extreme precipitation across Antarctica from 1979 to the present-day. Our approach uses precipitation from ERA5 reanalysis to identify trends and precipitation output from the single-forcing and all-forcing large ensembles performed using the fully-coupled global climate model Community Earth System Model 2 (CESM2) to undertake the D&A analysis and identify the role of different external climate forcings versus internal climate variability.

2 Data and Methods

2.1 Datasets

In situ measurements of precipitation over Antarctica are extremely scarce and difficult to make due to the challenging remote environment and difficulties distinguishing between falling and wind-driven snow (Pritchard, 2021). Therefore, we use hourly precipitation data from the ERA5 reanalysis (Hersbach et al., 2020) at a horizontal resolution of 0.25° as the best estimate of present-day conditions in Antarctica as this provides complete spatial and temporal coverage of this region for the period of interest. ERA5 precipitation has been used previously in studies examining daily precipitation over Antarctica (Vignon et al., 2021; Carter et al., 2022; Tewari et al., 2022) and for extreme event analysis (Min Xu et al., 2024). However, for this study we only use data from 1979 to 2023 (45 years), as prior to this period there were relatively few satellite observations over the Southern Ocean and Antarctica, which are necessary to constrain the reanalysis (Bromwich et al., 2024).

As ARs are an important contributor to EPEs, we identify their occurrence using a 3-hourly AR detection dataset at a horizontal resolution of 0.5° from 1980 to 2023, derived from ERA5 reanalysis (Wille et al., 2025). Here, ARs are identified based on the meridional component of integrated vapor transport exceeding the 98th percentile of the monthly climatologies.

We also use daily precipitation output for the period 1979 to 2023 from the large ensemble simulations performed with the CESM2 model, which for the atmospheric component uses the 'low-top' version of the model (i.e., a top of 40 km and 32 vertical levels) and a horizontal resolution of 1°, as well as prescribed stratospheric ozone depletion (Danabasoglu et al., 2020; Simpson et al., 2023). The CESM2 large ensemble simulations were selected because of the relatively large number of members available and because the model has a relatively good representation of the surface climate of Antarctica (Dunmire et al., 2022), which are both crucial for the D&A analysis. We use CESM2 ensembles that consider all external forcings (ALL; 50 members) and span the period from 1850 to 2100 under CMIP6 (Coupled Model Intercomparison Project Phase 6) historical and SSP370 (Shared Socioeconomic Pathways, representing additional radiative forcing of 7 W m^{-2} by 2100) scenario for the future, i.e., forcings due to both anthropogenic (such as greenhouse gases and aerosols caused by human activities) and natural

https://doi.org/10.5194/egusphere-2025-4292
Preprint. Discussion started: 23 September 2025

(such as solar variability and volcanic eruptions) causes. In addition to this, we also use CESM2 ensembles that consider single-forcing and span the period from 1850 to 2050 (Simpson et al., 2023), which are simulations forced by greenhouse gases only (GHG; 15 members) and by anthropogenic aerosols only (AAER; 20 members). Here, the GHG and AAER concentrations are evolving in time in their respective simulations, while all other forcings are fixed at 1850 values. In the AAER ensemble, the aerosols included are from industrial, agricultural, household, and transportation-related sources but exclude any anthropogenic biomass burning sources (e.g., black carbon and soot). Finally, to assess internal variability we use the CESM2 pre-industrial 2000-year long control simulation (with forcings fixed at 1850 values). Note that there is no CESM2 single-forcing experiment for stratospheric ozone depletion available (Simpson et al., 2023), and thus the effects of the Antarctic ozone hole are not considered in our analysis.

2.2 Methods

Hourly ERA5 precipitation outputs are firstly re-gridded onto the CESM2 grid using an area-weighted averaging method, and then summed over 24-hour intervals to produce daily values. We then compute trends in total and extreme precipitation for ERA5 and the ALL, GHG, and AAER ensembles for the period 1979 to 2023. Here, precipitation days are defined as days with precipitation exceeding a threshold of 0.02 mm day^{-1}, and extreme precipitation as days with precipitation exceeding the 95^{th} percentile of all precipitation days over the period 1979 to 2023, following Swetha Chittella et al. (2022). These daily data are then annually aggregated to obtain an annual time-series of both total and extreme precipitation for ERA5 and each member of the ALL, GHG, and AAER ensembles from 1979 to 2023. These are subsequently used to calculate: i) the spatial distribution of statistically significant (90% confidence interval) linear trends of total and extreme precipitation over Antarctica from ERA5, and ii) statistically significant (90% confidence level) basin-averaged linear trends of total precipitation and extreme precipitation for Antarctica's 18 drainage basins from ERA5 (mapped using the Ice Sheet Mass Balance Inter-comparison (IMBIE) dataset shown in Fig. 1; Rignot et al., 2019), and iii) to what extent the total and extreme precipitation trends from ERA5 can detected and attributed to specific external forcings using the CESM2 ensembles.

To examine trends in AR-associated total and extreme precipitation, for a day during which an AR is present, we summed the 3-hourly precipitation values from the AR detection dataset over 24-hour intervals to produce daily AR-associated precipitation. AR-associated extreme precipitation is then calculated as days with precipitation exceeding the 95^{th} percentile of all precipitation days over the period 1980 to 2023. These daily data are then annually aggregated to obtain an annual time-series of both AR-associated total and extreme precipitation from 1980 to 2023. Following the approach of Maclennan et al. (2022), this was subsequently used to investigate: i) the spatial distribution of statistically significant (90% confidence interval) AR-associated total and extreme precipitation, and ii) the relative contribution of AR-associated total and extreme precipitation trends to the ERA5-based total and extreme precipitation trends (which required regridding the total and extreme precipitation from ERA5 onto the AR detection dataset grid).

https://doi.org/10.5194/egusphere-2025-4292
Preprint. Discussion started: 23 September 2025

Next, we assessed the ability of the ALL ensemble to capture the ERA5 trends in total and extreme precipitation for the Antarctic drainage basins that show statistically significant trends. Here, if the basin-averaged linear trends in total and extreme precipitation from the ALL ensemble are significant at the 90% level and consistent with the trends estimated by ERA5, then the ALL ensemble was judged to reproduce the ERA5-based trends for that basin. For the basins identified during this step, we subsequently conduct a preliminary analysis of the forcings associated with these trends by assessing the contribution of the trends simulated by the GHG and AAER ensembles to the trends in the ALL ensemble. This was primarily achieved by comparing probability density distributions for the precipitation trends for each of the basins from the ALL, GHG, and AAER ensembles, calculated using a kernel density estimation method (significant at the 90% confidence level).

We then apply a regression-based D&A technique for the selected drainage basins, referred to as optimal fingerprinting analysis (Allen and Stott, 2003; Ribes et al., 2013; Dong et al., 2020; Hobbs et al., 2020; Dalaiden et al., 2022), to further investigate to what extent the total and extreme precipitation trends from ERA5 can be formally associated with external forcing. In this method, a generalized linear regression model (based on a least-squares fitting framework) is used to calculate scaling factors (also known as regression-based coefficients) between ERA5 and combinations of the CESM2 ensembles, as well as the CESM2 pre-industrial control simulation to also consider internal climate variability. This method also provides confidence intervals associated with the scaling factors to represent uncertainty. If the scaling factor (and its confidence interval) is greater than zero, then the observed changes are outside the range of internal variability. We therefore conclude that the observed changes can only be explained by external forcing (Dong et al., 2020; Dalaiden et al., 2022). However, if the scaling factor (and its confidence interval) is greater than one, this implies that the model significantly underestimates the observed trends. While if the scaling factors (and their confidence intervals) are smaller than one and greater than zero, this implies that the model significantly overestimates these trends. Finally, if the lower bound of the confidence interval is smaller than or equal to zero, we cannot conclude a statistically impact of external forcing on the observed changes.

Using this method, detection is investigated by applying a one-signal analysis, where the basin-averaged total and extreme precipitation time-series from the ALL ensemble (along with internal variability) are regressed onto the ERA5 time-series, resulting in scaling factors (and confidence intervals) for ALL (Dalaiden et al., 2022). Following this, attribution is investigated by applying a three-signal analysis, where the basin-averaged total and extreme precipitation time-series from the ALL, GHG and AAER ensembles (along with internal variability) are regressed onto the ERA5 time-series (Dalaiden et al., 2022). This results in scaling factors (and confidence intervals) for GHG and AAER, and also all forcings other than greenhouse gases and anthropogenic aerosols, which is labelled OTHERS (Gillett et al., 2021; Dalaiden et al., 2022). Unlike the one-signal analysis, the three-signal analysis therefore allows assessment of the contributions of different forcing to the ERA5 changes. Here, the basin-averaged contribution of internal variability to total and extreme precipitation comes from the pre-industrial control simulation.

https://doi.org/10.5194/egusphere-2025-4292
Preprint. Discussion started: 23 September 2025

Both the one-signal and three-signal analysis were performed with a common number of members from each ensemble, which was therefore limited to 15, i.e., the number from the GHG ensemble, as this was less than both the ALL (50) and AAER (20) ensembles. However, the results from the one-signal analysis using all 50 members from the ALL ensemble were largely identical to using 15 members (not shown). Additionally, the one-signal analysis is not applied to single-forcing ensembles (e.g., GHG and AAER) because, by construction, it forces each ensemble to match against ERA5 and can therefore lead to an artificial attribution of the changes in ERA5 to forcings that cannot physically explain them.

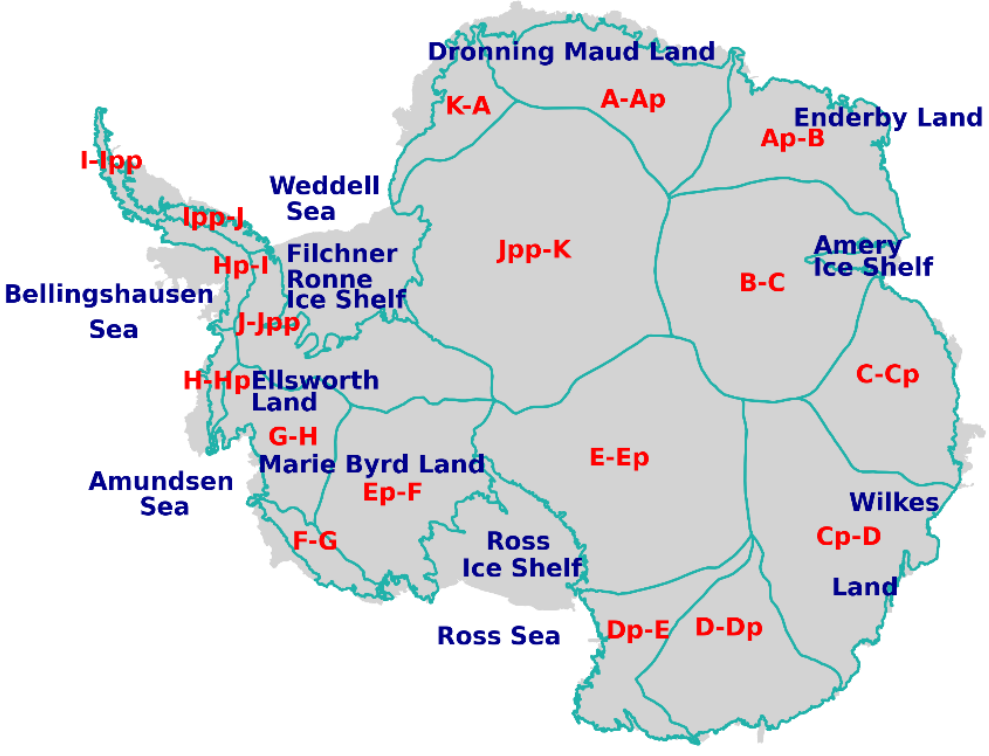

Figure 1: Map of Antarctica showing key regions of interest and the 18 major drainage basins, as defined in the IMBIE dataset (Rignot et al., 2019).

3 Results

3.1 Identification of precipitation trends

Figure 2 (a, e) shows annual trends in total and extreme precipitation from ERA5 from 1979 to 2023. This shows that broad positive trends for both total and extreme precipitation (up to 2 mm year^{-1}) are apparent from Ellsworth Land in West Antarctica to the Amery ice shelf in East Antarctica, while negative trends (up to -2 mm year^{-1}) are evident from Marie Byrd Land in West Antarctica to Wilkes Land in East Antarctica (see Fig. 1 for locations). However, for some of these regions, the trends

https://doi.org/10.5194/egusphere-2025-4292
Preprint. Discussion started: 23 September 2025

are statistically insignificant, with only Ellsworth Land, the Filchner-Ronne basin, Dronning Maud Land, Enderby Land, and the Amery Ice Shelf showing relatively large areas with significant positive trends, and only Marie Byrd Land and Wilkes Land showing relatively large areas with significant negative trends. Over the Antarctic Peninsula, the ERA5 trends in total and extreme precipitation differ in direction, with total precipitation increasing and extreme precipitation decreasing, although only the trends over the northern Antarctic Peninsula are significant.

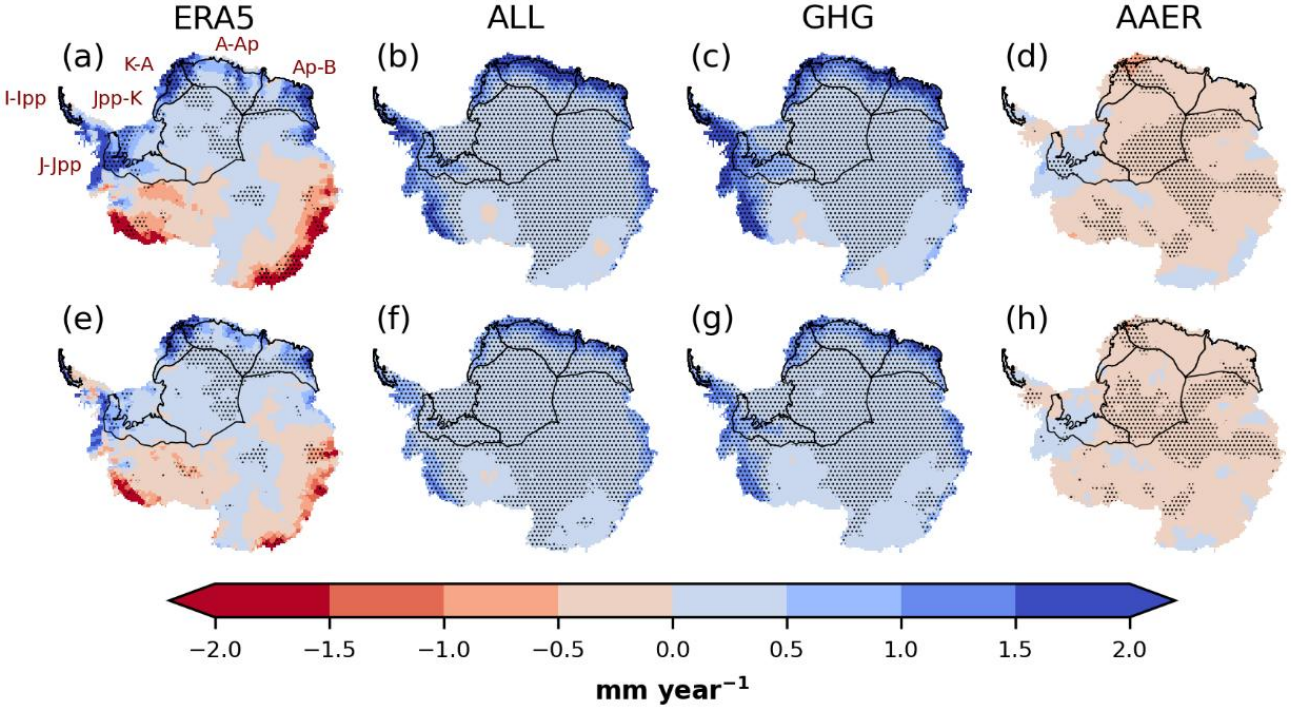

Figure 2: Annual trends in (a-d) total and (e-h) extreme precipitation over Antarctica for the period 1979 to 2023 (mm year^{-1}) from (a, e) ERA5 and the ensemble mean from the (b, f) ALL, (c, g) GHG, and (d, h) AAER ensembles. Stippling indicates regions where trends are statistically significant at the 90% confidence level. Also shown in panel (a) are the locations of the I-Ipp drainage basin in the Antarctic Peninsula, the J-Jpp basin in West Antarctica and the Jpp-K basin in East Antarctica (both part of Filchner-Ronne basin), and the K-A, A-Ap (both part of Dronning Maud Land), and Ap-B (Enderby Land) drainage basins in East Antarctica (outlined in black).

Within the regions showing positive ERA5-based trends, we identified six drainage basins that showed significant basin-averaged trends in both total and extreme precipitation (Figs. 2 and 3). These are basin I-Ipp in the Antarctic Peninsula, basins J-Jpp in West Antarctica and Jpp-K in East Antarctica (both part of the Filchner-Ronne basin), basins K-A and A-Ap in East Antarctica (both part of Dronning Maud Land), and basin Ap-B in East Antarctica (Enderby Land) (see Figs. 1 and 2 for locations). The basins J-Jpp, A-Ap, and Ap-B all have similar basin-averaged ERA5 trends of about 1 mm year^{-1} for total precipitation and 0.5 mm year^{-1} for extreme precipitation, whereas basins Jpp-K, K-A, and I-Ipp have trends of about 0.1, 1.5, and 5 mm year^{-1} for total precipitation respectively, and 0.1, 1, and 2.5 mm year^{-1} for extreme precipitation respectively (Fig. 3).

https://doi.org/10.5194/egusphere-2025-4292
Preprint. Discussion started: 23 September 2025

3.2 Detection of precipitation trends

Figure 2 (b, f) demonstrates that the ensemble mean of the ALL ensemble also shows significant positive trends for both total and extreme precipitation (up to 2 mm year^{-1}) from Ellsworth Land to the Amery ice shelf, which agree with ERA5. For example, it largely captures the spatial pattern and magnitude of the significant positive trends from ERA5 for total and extreme precipitation over Ellsworth Land, the Filchner-Ronne basin, Dronning Maud Land, Enderby Land, and the Amery ice shelf. Additionally, the ensemble mean from ALL also shows significant positive trends for total precipitation over the Antarctic Peninsula, which agree with significant positive trends from ERA5. By contrast, the ensemble mean from ALL shows positive trends in total and extreme precipitation over Marie Byrd Land and the western section of Wilkes Land, and positive trends for extreme precipitation over the Antarctic Peninsula, which disagree with ERA5. However, some differences in trends between the ALL ensemble and ERA5 results are to be expected as the ALL results are based on an ensemble of model means, which would therefore artificially reduce the contribution from internal variability, i.e., the ALL signal is only from forced variability, while the ERA5 signal is a combination of both internal and forced variability.

For the six drainage basins that are identified as having significant positive trends in both total and extreme precipitation from ERA5, Fig. 3 shows that for five of them (J-Jpp in West Antarctica, and Jpp-K, A-Ap, Ap-B, and K-A in East Antarctica) that: i) the basin-averaged trends from the ensemble mean of the ALL ensemble are close to the ERA5 trends, and ii) the range of the basin-averaged ALL trends from the different members includes the ERA5 trends (although this is less apparent for basin K-A). We therefore identify these five basins as having ALL trends that are in good agreement with ERA5 trends, and focus on these basins for the rest of our analysis. By contrast, the ERA5 trend for the remaining basin (I-Ipp in the Antarctic Peninsula) is outside the range of the ALL trends from the different members, and therefore is not considered for further analysis. Additionally, to further compare the basin-averaged trends between ERA5 and the ensemble mean of the ALL ensemble, Fig. 4 shows their time-series of total and extreme precipitation from 1979 to 2023 for our five selected basins. Consistent with Fig. 3, this shows broadly similar positive trends for all five basins for both ERA5 and ALL (although this is again less apparent for basin K-A). However, Fig. 4 also shows that the ensemble mean of ALL shows considerably higher precipitation amounts than ERA5 over the basins at the start of the period analysed, reflecting a mean state bias in the CESM2 model (Dunmire et al., 2022).

https://doi.org/10.5194/egusphere-2025-4292
Preprint. Discussion started: 23 September 2025

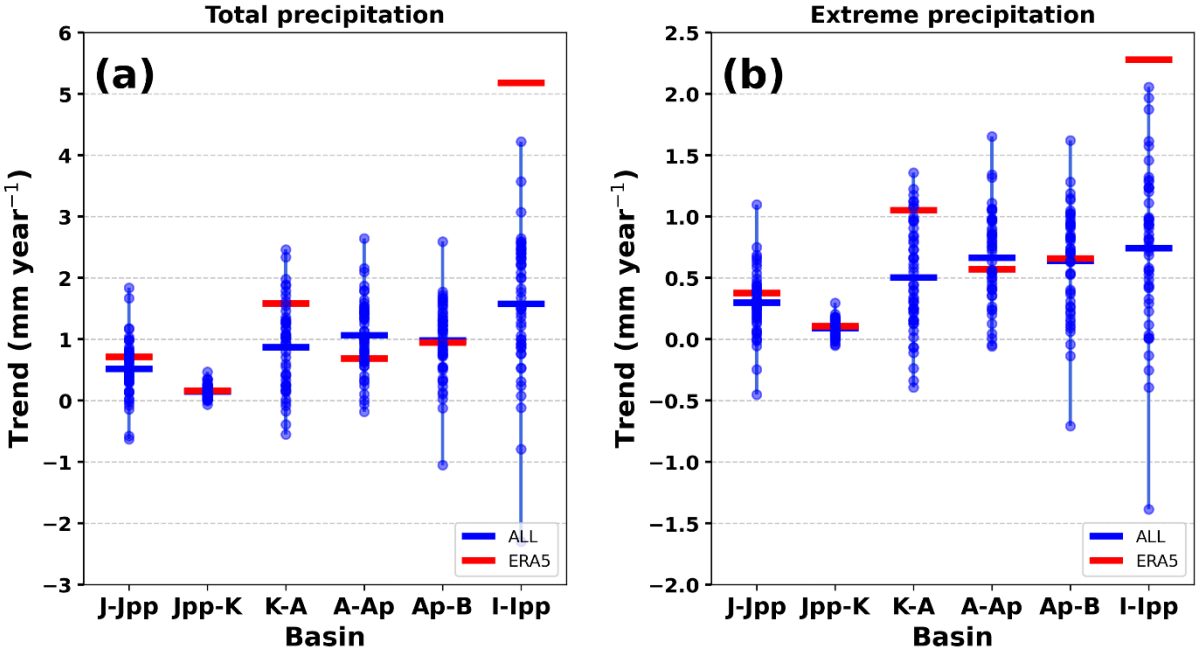

Figure 3: Basin-averaged annual trends in (a) total and (b) extreme precipitation for drainage basins J-Jpp, Jpp-K, K-A, A-Ap, Ap-B, and I-Ipp for the period 1979 to 2023 (mm year^{-1}) from ERA5 (thick red line) and the ensemble mean from the ALL ensemble (thick blue line). Also shown are the basin-averaged trends from the different members (50) of the ALL ensemble (filled blue circles). The trends are statistically significant with a 90% confidence level.

Figure 5 presents the one-signal D&A results for total and extreme precipitation across the five selected basins, based on regression of the ALL ensemble onto ERA5. This shows: i) scaling factors of around 0.6 to 0.8 for both total and extreme precipitation, and ii) relatively small confidence intervals, with total precipitation showing narrower intervals than extreme precipitation. Since the scaling factors are greater than zero and the confidence intervals are relatively small, this suggests with high confidence that the signal from the ALL ensemble is detectable in ERA5, i.e., supporting the results from Figs. 2 and 3. Additionally, because the scaling factors are less than one, this suggests that the ALL ensemble tends to overestimate the trends apparent in ERA5. Also, the slightly narrower intervals for total precipitation suggests that the influence of internal variability is larger for extreme precipitation compared to total precipitation.

https://doi.org/10.5194/egusphere-2025-4292
Preprint. Discussion started: 23 September 2025

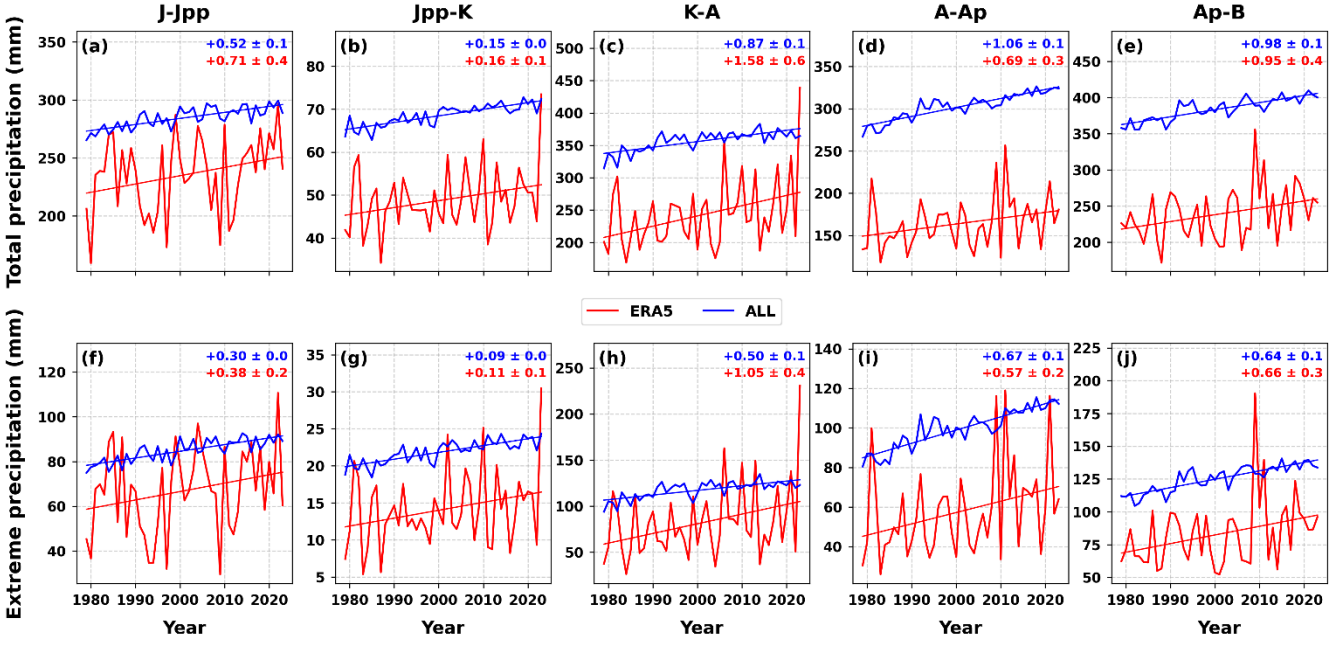

Figure 4: Times series of basin-averaged annual (a-e) total and (f-j) extreme precipitation (mm) for drainage basins J-Jpp, Jpp-K, K-A, A-Ap, and Ap-B from 1979 to 2023 from ERA5 (red) and the ensemble mean of the ALL ensemble (blue). Linear trends (statistically significant at 90% confidence level) for ERA5 and ALL are represented by the red and blue lines, respectively. Each panel also shows the linear trend and the standard error (mm year^{-1}).

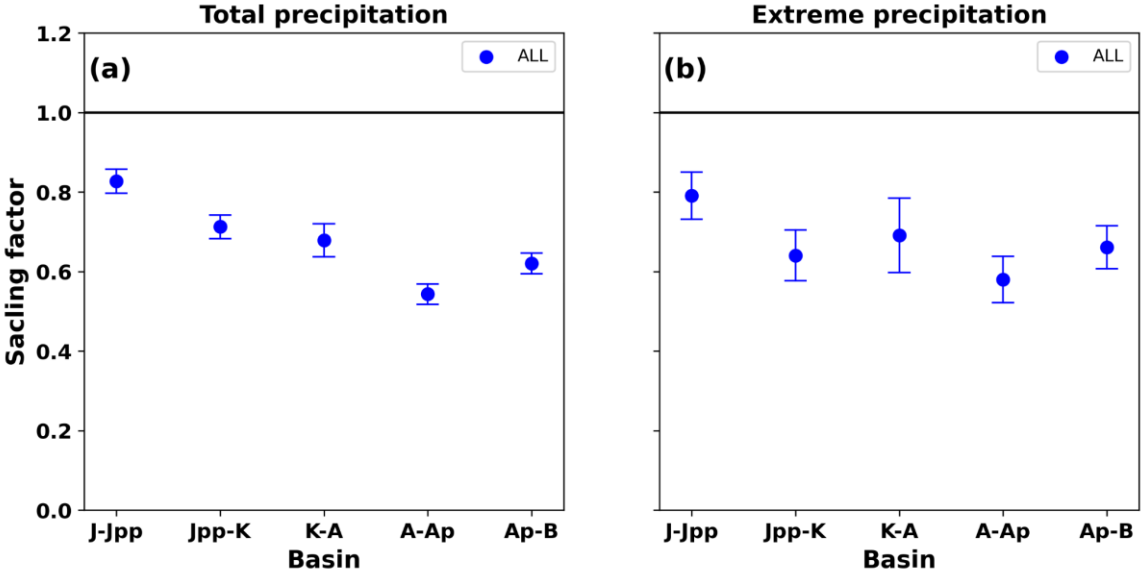

Figure 5: One-signal estimates of basin-averaged scaling factors (solid blue circles) for annual (a) total and (b) extreme precipitation for drainage basins J–Jpp, Jpp–K, K–A, A–Ap, and Ap–B for the period 1979 to 2023 based on regressing the ALL ensemble against ERA5. The error bars denote the 90% confidence intervals and the horizontal line indicates a scaling factor of one.

https://doi.org/10.5194/egusphere-2025-4292
Preprint. Discussion started: 23 September 2025

Table 1: Basin-averaged ensemble mean annual trends in total and extreme precipitation (mm year^{-1}) for drainage basins J-Jpp, Jpp-K, K-A, A-Ap, and Ap-B for the period 1979 to 2023 (mm year^{-1}) from the ALL, GHG, and AAER ensembles. Trends that are statistically significant at the 90% confidence level are shown in bold.

	ALL		GHG		AAER	
Basins	Total precipitation	Extreme precipitation	Total precipitation	Extreme precipitation	Total precipitation	Extreme precipitation
J-Jpp	**0.52**	**0.30**	**0.77**	**0.46**	0.08	0.03
Jpp-K	**0.15**	**0.09**	**0.12**	**0.13**	**-0.04**	**-0.04**
K-A	**0.87**	**0.50**	**1.13**	**0.84**	**-0.24**	**-0.15**
A-Ap	**1.06**	**0.67**	**0.86**	**0.56**	-0.17	-0.09
Ap-B	**0.98**	**0.64**	**1.2**	**0.76**	-0.09	-0.12

3.3 Attribution of precipitation trends

An initial assessment of the contribution from different external forcings to the positive trends for both total and extreme precipitation from the ALL ensemble (that are in agreement with ERA5) was made by comparing these trends with the ensemble mean from the GHG and AAER ensembles (Fig. 2). These results show that the ensemble mean trends in total and extreme precipitation from the GHG ensemble are in good agreement with those from the ALL ensemble over much of Antarctica, i.e., indicating that greenhouse gas forcing is the primary driver of the positive trends in the ALL ensemble. For example, the GHG ensemble captures the positive trends from Marie Byrd Land to the western section of Wilkes Land that are apparent in ALL. By contrast, the trends of the ensemble mean of the AAER ensemble are mostly negative for total and extreme precipitation over Antarctica, although areas that show significant trends are rather patchy, i.e., indicating that the effects of increased anthropogenic aerosols tend to offset the positive trends from increased greenhouse gases.

To assess the contribution from different external forcings to the positive trends for both total and extreme precipitation from the ALL ensemble for the five target basins, Table 1 compares basin-averaged ensemble mean trends from the ALL, GHG, and AAER ensembles for each of these. For total precipitation, the basin-averaged ensemble mean trends of the GHG ensemble exceeds the ALL trends in three out of the five basins (J-Jpp, K-A, and Ap-B), with values ranging from around 0.8 to 1.2 mm year^{-1} for GHG and from 0.5 to 1 mm year^{-1} for ALL. While for extreme precipitation, the basin-averaged ensemble mean trends of the GHG ensemble exceeds the ALL trends in four out of five basins (J-Jpp, Jpp-K, K-A, and Ap-B), with values ranging from around 0.5 to 0.8 mm year^{-1} for GHG and from 0.1 to 0.6 mm year^{-1} for ALL. By contrast, the basins show negative AAER trends, confirming that increased anthropogenic aerosols largely offset the positive GHG trends (although only the trends for basins Jpp-K and K-A are significant). For example, the AAER trends for total and extreme precipitation are both -0.04 mm year^{-1} for the Jpp-K basin, while the GHG trends are 0.12 and 0.14 mm year^{-1}, respectively, i.e., the magnitude of the AAER trends are around a third of the GHG trends. While the AAER trends are -0.24 and -0.15 mm year^{-1}

https://doi.org/10.5194/egusphere-2025-4292
Preprint. Discussion started: 23 September 2025

for total and extreme precipitation for basin K-A, respectively, and 1.13 and 0.84 mm year^{-1} for GHG, i.e., the magnitude of the AAER trends are roughly one-fifth of the GHG trends. This therefore further indicates that greenhouse gas forcing is the primary driver of the positive precipitation trends in the five basins, and that these trends are partially offset by the effects of increased anthropogenic aerosols.

The importance of greenhouse gas forcing for producing the positive trends in total and extreme precipitation over the five selected basins is also evident from probability distribution functions of the trends from the ALL, GHG, and AAER ensembles, which shows considerable similarities between the distributions for the GHG and ALL trends (Fig. 6). The distribution of the AAER trends also confirms the offsetting effect of anthropogenic aerosols for the Jpp-K and K-A basins, where AAER distributions are skewed towards negative values. By contrast, for the remaining basins the AAER distributions are more mixed, with both positive and negative trends.

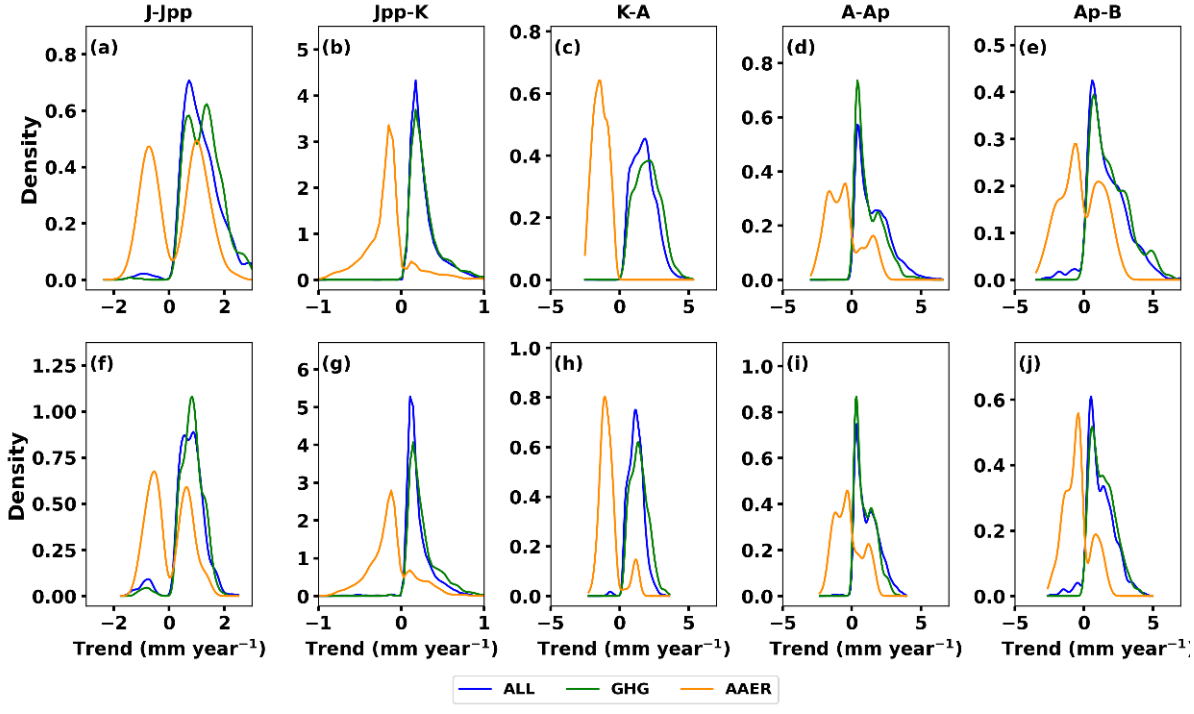

Figure 6: Probability density functions of annual trends in (a-e) total and (f-j) extreme precipitation for drainage basins J-Jpp, Jpp-K, K-A, A-Ap and Ap-B for the period 1979 to 2023 (mm year^{-1}) from the ALL (blue), GHG (green), and AAER (orange) ensembles. The results are based only on annual trends from grid points that are statistically significant at the 90% confidence level.

https://doi.org/10.5194/egusphere-2025-4292
Preprint. Discussion started: 23 September 2025

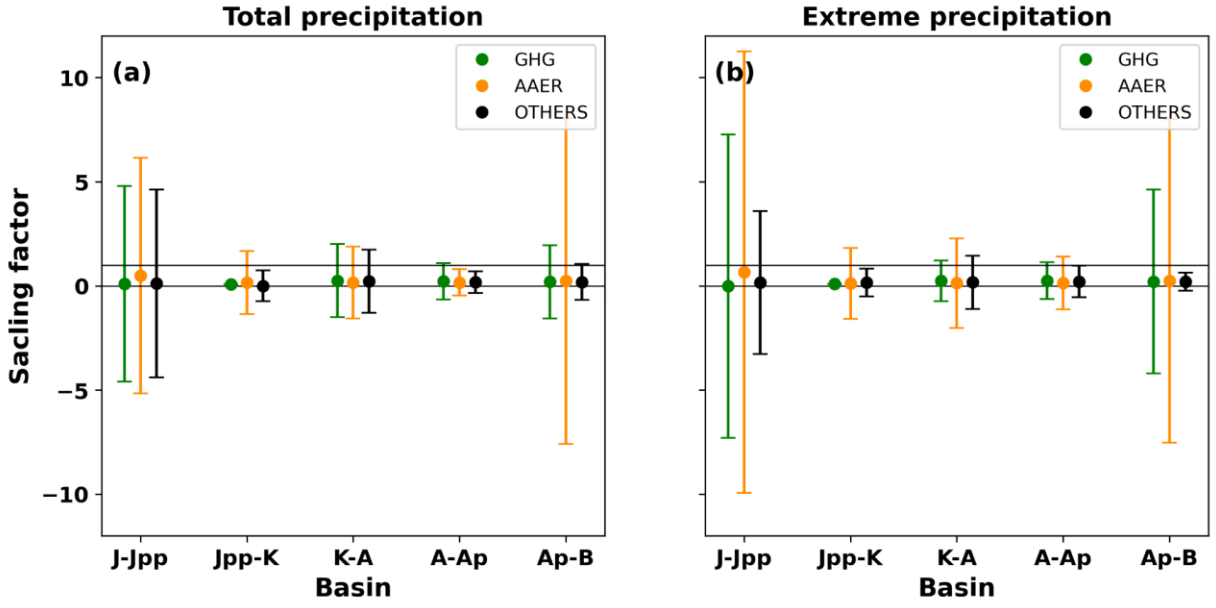

Figure 7: As Fig. 5, but showing three-signal estimates of basin-averaged scaling factors for annual (a) total and (b) extreme precipitation for drainage basins J–Jpp, Jpp–K, K–A, A–Ap, and Ap–B for the period 1979 to 2023 based on regressing the GHG ensemble (solid green circles), AAER ensemble (solid orange circles), and OTHERS (solid black circles; all forcings other than greenhouse gases and anthropogenic aerosols) against ERA5. The error bars denote the 90% confidence intervals and the horizontal line indicates a scaling factor of one.

Figure 7 presents the three-signal D&A results for total and extreme precipitation across the five selected basins, based on regression of the ALL, GHG, and AAER ensembles against ERA5, which produces scaling factors for GHG, AAER, and OTHERS (i.e., all forcings other than greenhouse gases and anthropogenic aerosols). Here, the scaling factors were all associated with large confidence intervals, generally ranging from -7 to 7 for GHG, -10 to 10 for AAER and -5 to 5 for OTHERS. This indicates very low confidence in the obtained regression. Therefore, the signals from the GHG and AAER ensembles (and OTHERS) cannot be considered statistically significant for either total or extreme precipitation. One exception is basin Jpp–K, where the GHG signal is detected because the lower bound of the confidence interval is greater than zero. However, this result still lacks consistency as the upper bound of the confidence interval is less than one, which suggests that GHG tends to overestimate the trends apparent in ERA5.

https://doi.org/10.5194/egusphere-2025-4292
Preprint. Discussion started: 23 September 2025

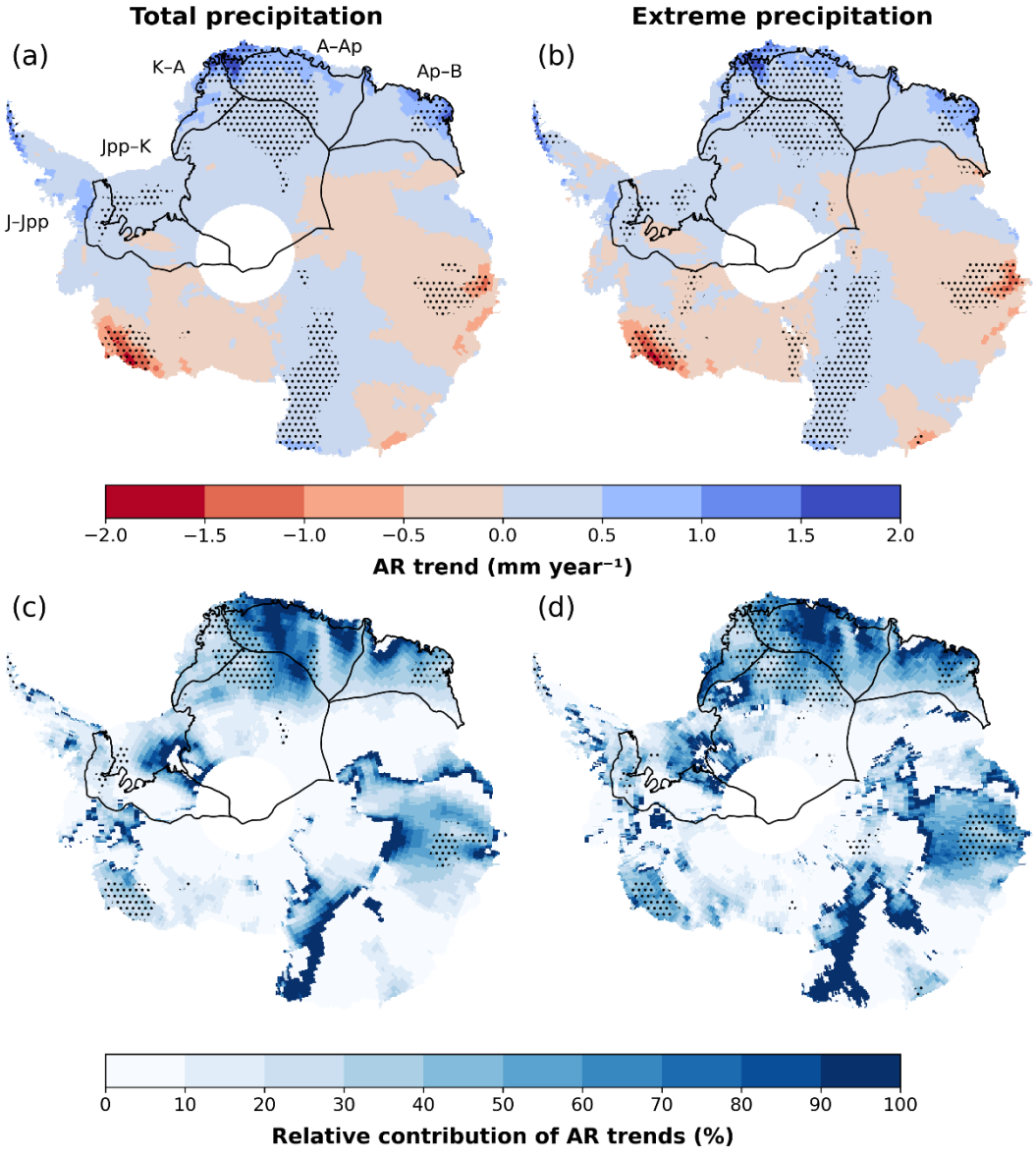

Figure 8: Annual trends in AR-associated (a) total and (b) extreme precipitation over Antarctica for the period 1980 to 2023 (mm year^{-1}) from the AR detection dataset. Also shown are the relative contribution of the (c) AR-associated total precipitation trend to the ERA5-based total precipitation trend (%), and the (d) AR-associated extreme precipitation trend to the ERA5-based extreme precipitation trend (%). Stippling indicates regions where trends are statistically significant at the 90% confidence level. Also shown in panel (a) are the locations of drainage basins J-Jpp, Jpp-K, K-A, A-Ap and Ap-B.

3.4 Role of atmospheric rivers in driving precipitation trends

Finally, to assess the role of ARs in driving the positive trends of total and extreme precipitation that are apparent in ERA5 over these five basins (Figs. 2 and 3), we also show the annual trends in AR-associated total and extreme precipitation from 1980 to 2023 (Fig. 8a, b), as well as the relative contribution of these trends to the total and extreme precipitation trends from

https://doi.org/10.5194/egusphere-2025-4292
Preprint. Discussion started: 23 September 2025

ERA5 (Fig. 8c, d). The results show broadly significant positive trends in AR-associated total and extreme precipitation over the basins considered, with trends around 0.5 mm year^{-1} over basins J-Jpp and Jpp-K and up to 2 mm year^{-1} over basins K-A, A-Ap, and Ap-B. Additionally, the relative contribution of the AR trends to the ERA5-based total and extreme precipitation trends has increased across all five basins, with values of 10 to 40% over sections of basins J-Jpp, Jpp-K, and K-A, and up to 100% over sections of basins A-Ap and Ap-B.

4 Discussion

Our initial attribution analysis of total and extreme precipitation trends showed good agreement between the trends from the ensemble mean of the ALL and GHG ensembles for our five target basins (Figs. 2 and 6, Table 1), indicating that greenhouse gases are the primary driver of the present-day trends in total and extreme precipitation over these basins. Additionally, our initial attribution analysis also suggests that increases in anthropogenic aerosol emissions can oppose / offset the increases in precipitation from increased greenhouse gases over our five basins (Figs. 2 and 6, Table 1). However, the three-signal regression-based D&A analysis using the ALL, GHG and AAER ensembles (resulting in scaling factors for GHG, AAER, and OTHERS) was unable to provide robust attribution for total or extreme precipitation to any specific single-forcing, including increased greenhouse gases (Fig. 7). This inconsistency between these results demonstrates that formally detecting the fingerprint of anthropogenic forcing on recent Antarctic precipitation changes remains highly challenging (Previdi and Polvani, 2016; Dalaiden et al., 2022).

For example, one of the main challenges in detecting a trend in total and extreme precipitation is separating the signal from forced variability and internal variability, which is exacerbated in Antarctica by its climate being particularly characterized by strong internal variability (Jones et al., 2016a; Previdi and Polvani, 2016; Stenni et al., 2017). Thus, detection of the signal in ERA5 in the ALL ensemble using the one-signal regression-based D&A analysis is confined to five drainage basins (Fig. 5) where the forced signal emerges more clearly above internal variability, with four of the five basins located in East Antarctica and the other in West Antarctica. This agrees with Casado et al. (2023), who found weaker multi-decadal variability in East Antarctic ice cores compared to West Antarctic, i.e., the relatively weaker internal multi-decadal variability in East Antarctica likely increases the signal-to-noise ratio, and enables a more robust detection of the forced signal in this region. Additional challenges also include that the three-signal analysis has more degrees of freedom than the one-signal analysis, making it more uncertain, and that there are likely larger uncertainties with forcings such as anthropogenic aerosols, as well as their modelled response (Jones et al., 2016b).

We also showed that the trends in total and extreme precipitation over the five target basins can be linked to increasing ARs (Fig. 8). This provides physical support for the analysis, highlighting the consistency between the identification of the trends and the underlying dynamical drivers. This result is also consistent with previous results that suggested that ARs contribute up to 20% of total precipitation in East Antarctica (Wille et al., 2021, 2025; Maclennan et al., 2022), and as much as 50 to 70%

https://doi.org/10.5194/egusphere-2025-4292
Preprint. Discussion started: 23 September 2025

of extreme precipitation (Wille et al., 2021, 2025; Simon et al., 2024). The increased ARs are likely associated with anomalous northerly airflow, combined with increased atmospheric moisture from warmer oceans, which could be linked to recent regional climate changes such as sea-ice loss in the East Antarctic sector and a strengthening of the low-pressure system off the East Antarctic coast (Goosse et al., 2024). Moreover, additional anomalous transport from the midlatitudes through Rossby-wave teleconnections could also be a factor (Wille et al., 2025). Moreover, future increases in greenhouse gas concentrations are expected to strengthen Antarctic total and extreme precipitation by causing warmer atmospheric conditions (leading to more moisture, via the Clausius-Clapeyron relation) and a reduction in sea-ice (Frieler et al., 2015; Lenaerts et al., 2016; Previdi and Polvani, 2016; Kittel et al., 2021; Vignon et al., 2021; Zhu et al., 2023; Nicola et al., 2023).

Moreover, its noteworthy that the effects of increased greenhouse gas emissions are generally considered to be a positive trend in the Southern Annular Mode (SAM) (Kushner et al., 2001; Arblaster and Meehl, 2006), which corresponds to stronger, poleward-shifted westerlies around Antarctica, resulting in reduced temperatures (and precipitation) over East Antarctica (Thompson and Solomon, 2002). While increased anthropogenic aerosol emissions are generally considered to correspond to the opposite effects (Gillett et al., 2013; Pope et al., 2020). Based on this, as greenhouse gases are the dominant driver of the present-day trends, a decrease in precipitation and extreme precipitation over our five target basins (four of which are in East Antarctica) would be expected, rather than an increase. However, one reason for this contradiction may be a reversal in the relationship between SAM and temperature anomalies across East Antarctica during the twenty-first century, which occurred in response to anomalous high pressure over East Antarctica (Marshall et al., 2013). This anomalous circulation would result in increased northerly airflow into East Antarctica, i.e., consistent with our results showing increased precipitation and intensification of ARs.

However, because the CESM2 ensembles that consider single-forcing do not include stratospheric ozone depletion, the influence of the Antarctic ozone hole was not specifically considered in our attribution analysis (Dalaiden et al., 2022). This is a primary driver of summertime atmospheric circulation changes in the Southern hemisphere from around 1980 onwards (Thompson and Solomon, 2002; Polvani et al., 2011; Orr et al., 2021), which Dalaiden et al. (2022) showed was partly responsible for recent increases in precipitation over West Antarctica. Furthermore, the combined and potentially non-linear effects of different forcings is also likely important for representing precipitation, and especially for extreme precipitation where linear assumptions are least valid (Meehl et al., 2003; Pope et al., 2020).

Finally, in our study, although we rely primarily on ERA5 as the best estimate of recent precipitation changes, we did consider using precipitation outputs from high-resolution regional climate model simulations (e.g., Deb et al., 2018; Mottram et al., 2021; Carter et al., 2022; Orr et al., 2023; Gilbert et al., 2025) which dynamically downscale ERA5 to a horizontal resolution of 0.1°. Such datasets are generally better suited to represent the critical interactions between atmospheric flows and the complex coastal orography that influences precipitation, and especially extreme events (Carter et al., 2022; Orr et al., 2023;

https://doi.org/10.5194/egusphere-2025-4292
Preprint. Discussion started: 23 September 2025

Gilbert et al., 2025). However, since our methodology required regridding to the coarser CESM2 grid (horizontal resolution of 1°), the added value from the downscaling was effectively lost, and no systematic advantage was gained compared to ERA5.

5 Conclusions

This study confirms a statistically significant increase in both total and extreme precipitation (up to 2 mm year^{-1}) across six drainage basins in Antarctica from 1979 to 2023, based on ERA5 reanalysis. These are basin I-Ipp in the Antarctic Peninsula, basin J-Jpp in West Antarctica and basin Jpp-K in East Antarctica (both part of Filchner-Ronne basin), basins K-A and A-Ap in East Antarctica (both part of Dronning Maud Land), and basin Ap-B in East Antarctica (Enderby Land). For five of these six basins (J-Jpp, Jpp-K, A-Ap, Ap-B, and K-A) the total and extreme precipitation trends from the ALL ensemble are in good agreement with those from ERA5, i.e., suggesting that a combination of both anthropogenic and natural forcings, along with internal variability are responsible for the present-day trends in total and extreme precipitation over these basins. This was confirmed using a regression-based D&A technique, based on the regression of the ALL ensemble against ERA5. The results also showed that a substantial portion of the ERA5-based trends in both total and extreme precipitation for these five basins are from a contemporaneous increase in precipitation from ARs, which provides additional physical support for the identification of the trends.

The study further showed that the trends in both total and extreme precipitation for these five basins from the GHG ensemble are in good agreement with those from the ALL ensemble, i.e., indicating that increased greenhouse gases are the primary driver of the positive precipitation trends over these basins. In contrast, trends from the AAER ensemble are generally negative and smaller in magnitude than the GHG ensemble trends, i.e., indicating that the effects of increased anthropogenic aerosol emissions slightly offset the effects of increased greenhouse gases. However, regressing the ALL, GHG, and AAER ensembles against ERA5 did not yield robust attribution to any specific forcing for either total or extreme precipitation, which is likely due to limitations such as the relatively small ensemble size of the simulations.

Code and data availability

The code used in this study can be obtained from the corresponding author upon reasonable request. Precipitation output from the ERA5 reanalysis dataset is publicly available through the Copernicus Climate Data Store: https://cds.climate.copernicus.eu/datasets/reanalysis-era5-single-levels?tab=overview. Precipitation output from the CESM2 ensembles with all external forcings are available at: https://rda.ucar.edu/datasets/d651056/. Precipitation output from the CESM2 ensembles with single-forcings are available at: https://rda.ucar.edu/datasets/d651055/dataaccess/#. Precipitation output from the CESM2 pre-industrial control simulation are available at: https://www.earthsystemgrid.org/dataset/ucar.cgd.cesm2.b.e21.B1850.f09_g17.CMIP6-

https://doi.org/10.5194/egusphere-2025-4292
Preprint. Discussion started: 23 September 2025

piControl.001.atm.proc.daily_ave.PRECT.html. The AR detection dataset derived from ERA5 is available at: https://zenodo.org/records/15830634.

Author contributions

SPSC designed the study and, together with PD and AO, conceptualized it. SPSC carried out the primary analysis with support from PD, AO, and QD. SPSC and AO were primarily responsible for writing the manuscript, with additions from PD and QD.

Competing interests

The corresponding author affirms that none of the authors have any financial or personal conflicts of interest to disclose.

Acknowledgement

The authors would like to thank Jonathan Wille for his advice on using the AR detection dataset.

Financial support

AO received support from the European Union's Horizon 2020 funded project PolarRES (Polar Regions in the Earth System; Grant No. 101003590) and the Natural Environment Research Council funded project PICANTE (Processes, Impacts and Changes of ANTarctic Extreme weather; Grant No. NE/Z503356/1). SPSC and PD received funding from the Indian Institute of Technology Kharagpur and the Ministry of Education, Government of India. QD received support from European Union's Horizon 2020 research and innovation programme under the Marie Skłodowska-Curie grant agreement 101149188.

References

Adusumilli, S., A Fish, M., Fricker, H. A., & Medley, B. (2021). Atmospheric river precipitation contributed to rapid increases in surface height of the west Antarctic ice sheet in 2019. *Geophysical Research Letters*, *48*(5), e2020GL091076. https://doi.org/10.1029/2020GL091076

Arblaster, J. M., & Meehl, G. A. (2006). Contributions of external forcings to southern annular mode trends. *Journal of climate*, *19*(12), 2896-2905. https://doi.org/10.1175/JCLI3774.1

Allen, M. R., & Stott, P. A. (2003). Estimating signal amplitudes in optimal fingerprinting, Part I: Theory. *Climate Dynamics*, *21*, 477-491. https://doi.org/10.1007/s00382-003-0313-9

Banwell, A. F., and D. R. MacAyeal, 2015: Ice-shelf fracture due to viscoelastic flexure stress induced by fill/drain cycles of supraglacial lakes. *Antarct. Sci.*, **27**, 587–597, https://doi.org/10.1017/S0954102015000292.

Bintanja, R., van Oldenborgh, G. J., Drijfhout, S. S., Wouters, B., & Katsman, C. A. (2013). Important role for ocean warming and increased ice-shelf melt in Antarctic sea-ice expansion. *Nature Geoscience*, *6*(5), 376-379. https://doi.org/10.1038/ngeo1767

Blanchard-Wrigglesworth, E., Cox, T., Espinosa, Z. I., & Donohoe, A. (2023). The largest ever recorded heatwave—Characteristics and attribution of the Antarctic heatwave of March 2022. Geophysical Research Letters, 50(17), e2023GL104910. https://doi.org/10.1029/2023GL104910

Boening, C., Lebsock, M., Landerer, F., & Stephens, G. (2012). Snowfall-driven mass change on the East Antarctic ice sheet. Geophysical Research Letters, 39, L21501. https://doi.org/10.1029/2012GL053316

Bromwich, D. H., Ensign, A., Wang, S. H., & Zou, X. (2024). Major artifacts in ERA5 2-m air temperature trends over Antarctica prior to and during the modern satellite era. Geophysical Research Letters, 51(21), e2024GL111907. https://doi.org/10.1029/2024GL111907

Carter, J., A. Leeson, A. Orr, C. Kittel, J. Melchior van Wessem (2022), Variability in Antarctic surface climatology across region climate models and reanalysis datasets, The Cryosphere, 16, 3815–3841, https://doi.org/10.5194/tc-16-3815-2022

Casado, M., Hébert, R., Faranda, D., & Landais, A. (2023). The quandary of detecting the signature of climate change in Antarctica. Nature Climate Change, 13(10), 1082-1088. https://doi.org/10.1038/s41558-023-01791-5

Connolley, W. M. (1997). Variability in annual mean circulation in southern high latitudes. Climate Dynamics, 13, 745-756. https://doi.org/10.1007/s003820050195

Dalaiden, Q., Schurer, A. P., Kirchmeier-Young, M. C., Goosse, H., & Hegerl, G. C. (2022). West Antarctic surface climate changes since the mid-20th century driven by anthropogenic forcing. Geophysical Research Letters, 49(16), e2022GL099543. https://doi.org/10.1029/2022GL099543

Danabasoglu, G., Lamarque, J. F., Bacmeister, J., Bailey, D. A., DuVivier, A. K., Edwards, J., ... & Strand, W. G. (2020). The community earth system model version 2 (CESM2). Journal of Advances in Modeling Earth Systems, 12(2), e2019MS001916. https://doi.org/10.1029/2019MS001916

Davison, B. J., Hogg, A. E., Rigby, R., Veldhuijsen, S., van Wessem, J. M., van den Broeke, M. R., ... & Dutrieux, P. (2023). Sea level rise from West Antarctic mass loss significantly modified by large snowfall anomalies. Nature Communications, 14(1), 1479. https://doi.org/10.1038/s41467-023-36990-3

Deb, P., Orr, A., Bromwich, D. H., Nicolas, J. P., Turner, J., & Hosking, J. S. (2018). Summer drivers of atmospheric variability affecting ice shelf thinning in the Amundsen Sea Embayment, West Antarctica. *Geophysical Research Letters*, *45*(9), 4124-4133. https://doi.org/10.1029/2018GL077092

Dong, S., Sun, Y., & Li, C. (2020). Detection of human influence on precipitation extremes in Asia. Journal of Climate, 33(12), 5293-5304. https://doi.org/10.1175/JCLI-D-19-0371.1

Dong, S., Sun, Y., Li, C., Zhang, X., Min, S. K., & Kim, Y. H. (2021). Attribution of extreme precipitation with updated observations and CMIP6 simulations. Journal of Climate, 34(3), 871-881. https://doi.org/10.1175/JCLI-D-19-1017.1

https://doi.org/10.5194/egusphere-2025-4292
Preprint. Discussion started: 23 September 2025

Donat, M. G., Alexander, L. V., Yang, H., Durre, I., Vose, R., Dunn, R. J., ... & Kitching, S. (2013). Updated analyses of temperature and precipitation extreme indices since the beginning of the twentieth century: The HadEX2 dataset. Journal of Geophysical Research: Atmospheres, 118(5), 2098-2118. https://doi.org/10.1002/jgrd.50150

Dunn, R. J., Alexander, L. V., Donat, M. G., Zhang, X., Bador, M., Herold, N., ... & Bin Hj Yussof, M. N. A. (2020). Development of an updated global land in situ-based data set of temperature and precipitation extremes: HadEX3. Journal of Geophysical Research: Atmospheres, 125(16), e2019JD032263. https://doi.org/10.1029/2019JD032263

Estrada, F., Perron, P., & Yamamoto, Y. (2023). Anthropogenic influence on extremes and risk hotspots. Scientific Reports, 13(1), 35. https://doi.org/10.1038/s41598-022-27220-9

Frieler, K., Clark, P. U., He, F., Buizert, C., Reese, R., Ligtenberg, S. R. M., et al. (2015). Consistent evidence of increasing Antarctic accumulation with warming. Nature Climate Change, 5(4), 348–352. https://doi.org/10.1038/nclimate2574

Favier, V., Krinner, G., Amory, C., Gallée, H., Beaumet, J., & Agosta, C. (2017). Antarctica-regional climate and surface mass budget. Current Climate Change Reports, 3(4), 303-315. https://doi.org/10.1007/s40641-017-0072-z

Fyke, J., Lenaerts, J. T. M., & Wang, H. (2017). Basin-scale heterogeneity in Antarctic precipitation and its impact on surface mass variability. The Cryosphere, 11(6), 2595–2609. https://doi.org/10.5194/tc-11-2595-2017

Gardner, A. S., Moholdt, G., Scambos, T., Fahnstock, M., Ligtenberg, S., van den Broeke, M., and Nilsson, J.: Increased West Antarctic and unchanged East Antarctic ice discharge over the last 7 years, The Cryosphere, 12, 521–547, https://doi.org/10.5194/tc-12-521-2018 , 2018.

Gillett, N. P., Stone, D. A., Stott, P. A., Nozawa, T., Karpechko, A. Y., Hegerl, G. C., ... & Jones, P. D. (2008). Attribution of polar warming to human influence, Nat. Geosci., 1, 750–754. https://doi.org/10.1038/ngeo338

Gehring, J., Vignon, É., Billault-Roux, A. C., Ferrone, A., Protat, A., Alexander, S. P., & Berne, A. (2022). Orographic flow influence on precipitation during an atmospheric river event at Davis, Antarctica. Journal of Geophysical Research: Atmospheres, 127(2), e2021JD035210. https://doi.org/10.1029/2021JD035210

Gillett, N. P., Stone, D. A., Stott, P. A., Nozawa, T., Karpechko, A. Y., Hegerl, G. C., ... & Jones, P. D. (2008). Attribution of polar warming to human influence. Nature Geoscience, 1(11), 750-754. https://doi.org/10.1038/ngeo338

Gillett, N. P., Fyfe, J. C., & Parker, D. E. (2013). Attribution of observed sea level pressure trends to greenhouse gas, aerosol, and ozone changes. Geophysical Research Letters, 40(10), 2302-2306. https://doi.org/10.1002/grl.50500

Gillett, N. P., Kirchmeier-Young, M., Ribes, A., Shiogama, H., Hegerl, G. C., Knutti, R., ... & Ziehn, T. (2021). Constraining human contributions to observed warming since the pre-industrial period. Nature Climate Change, 11(3), 207-212. https://doi.org/10.1038/s41558-020-00965-9

Gilbert, E., D. Pishniak, J. A. Torres, A. Orr, M. Maclennan, N. Wever, and K. Verro (2025), Extreme precipitation associated with atmospheric rivers over West Antarctic ice shelves: insights from kilometre-scale regional climate modelling, The Cryosphere, 19, 597–618, https://doi.org/10.5194/tc-19-597-2025.

Goosse, H., Dalaiden, Q., Feba, F., Mezzina, B., & Fogt, R. L. (2024). A drop in Antarctic sea ice extent at the end of the 1970s. Communications Earth & Environment, 5(1), 628. https://doi.org/10.1038/s43247-024-01793-x

https://doi.org/10.5194/egusphere-2025-4292
Preprint. Discussion started: 23 September 2025

Gorodetskaya, I. V., Tsukernik, M., Claes, K., Ralph, M. F., Neff, W. D., & Van Lipzig, N. P. (2014). The role of atmospheric rivers in anomalous snow accumulation in East Antarctica. Geophysical Research Letters, 41(17), 6199-6206. https://doi.org/10.1002/2014GL060881

Gu, C., Luo, Y., Liu, F., Lu, J., & Chen, Z. (2025). Increased Asian aerosols contribute to historical climate change in Antarctica. Geophysical Research Letters, 52(13), e2025GL114888. https://doi.org/10.1029/2025GL114888

Hersbach, H., Bell, B., Berrisford, P., Hirahara, S., Horányi, A., Muñoz-Sabater, J., ... & Thépaut, J. N. (2020). The ERA5 global reanalysis. Quarterly journal of the royal meteorological society, 146(730), 1999-2049. https://doi.org/10.1002/qj.3803

Hawkins, E., & Sutton, R. (2009). The potential to narrow uncertainty in regional climate predictions. Bulletin of the American Meteorological Society, 90(8), 1095-1108. https://doi.org/10.1175/2009BAMS2607.1,

Hobbs, W. R., Roach, C., Roy, T., Sallée, J. B., & Bindoff, N. (2021). Anthropogenic temperature and salinity changes in the Southern Ocean. Journal of Climate, 34(1), 215-228. https://doi.org/10.1175/JCLI-D-20-0454.1

Hosking, J. S., Orr, A., Marshall, G. J., Turner, J., & Phillips, T. (2013). The influence of the Amundsen–Bellingshausen Seas low on the climate of West Antarctica and its representation in coupled climate model simulations. Journal of Climate, 26(17), 6633-6648. https://doi.org/10.1175/JCLI-D-12-00813.1

IPCC, 2023: Climate Change 2023: Synthesis Report. Contribution of Working Groups I, II and III to the Sixth Assessment Report of the Intergovernmental Panel on Climate Change [Core Writing Team, H. Lee and J. Romero (eds.)]. IPCC, Geneva, Switzerland, 184 pp. https://doi.org/10.59327/IPCC/AR6-9789291691647.

Johnson, A., R. Hock, and M. Fahnestock, 2022: Spatial variability and regional trends of Antarctic Ice Shelf surface melt duration over 1979–2020 derived from passive microwave data. J. Glaciol., 68, 533–546, https://doi.org/10.1017/jog.2021.112.

Jones, G. S., Stott, P. A., & Mitchell, J. F. (2016a). Uncertainties in the attribution of greenhouse gas warming and implications for climate prediction. Journal of Geophysical Research: Atmospheres, 121(12), 6969-6992. https://doi.org/10.1002/2015JD024337

Jones, J. M., Gille, S. T., Goosse, H., Abram, N. J., Canziani, P. O., Charman, D. J., ... & Vance, T. R. (2016b). Assessing recent trends in high-latitude Southern Hemisphere surface climate. Nature Climate Change, 6(10), 917-926. https://doi.org/10.1038/nclimate3103

Kirchmeier-Young, M. C., Zwiers, F. W., & Gillett, N. P. (2017). Attribution of extreme events in Arctic sea ice extent. Journal of Climate, 30(2), 553-571. https://doi.org/10.1175/JCLI-D-16-0412.1

Kirchmeier-Young, M. C., & Zhang, X. (2020). Human influence has intensified extreme precipitation in North America. Proceedings of the National Academy of Sciences, 117(24), 13308-13313. https://doi.org/10.1073/pnas.1921628117

Kittel, C., Amory, C., Agosta, C., Jourdain, N. C., Hofer, S., Delhasse, A., ... & Fettweis, X. (2020). Diverging future surface mass balance between the Antarctic ice shelves and grounded ice sheet. The Cryosphere Discussions, 2020, 1-29. https://doi.org/10.5194/tc-15-1215-2021

Kromer, J. D., & Trusel, L. D. (2023). Identifying the impacts of sea ice variability on the climate and surface mass balance of West Antarctica. Geophysical Research Letters, 50(18), e2023GL104436. https://doi.org/10.1029/2023GL104436

https://doi.org/10.5194/egusphere-2025-4292
Preprint. Discussion started: 23 September 2025

514 Kuipers Munneke, P., and Coauthors, 2018: Intense winter surface melt on an Antarctic Ice Shelf. Geophys. Res. Lett., 45,
515 7615–7623, https://doi.org/10.1029/2018GL077899.
516 Kushner, P. J., Held, I. M., & Delworth, T. L. (2001). Southern Hemisphere atmospheric circulation response to global
517 warming. Journal of Climate, 14(10), 2238-2249. https://doi.org/10.1175/1520-0442(2001)014<0001:SHACRT>2.0.CO;2
518 Lai, C.-Y., J. Kingslake, M. G. Wearing, P.-H. Cameron Chen, P. Gentine, H. Li, J. J. Spergel, and J. M. van Wessem, 2020:
519 Vulnerability of Antarctica's ice shelves to meltwater-driven fracture. Nature, 584, 574–578, https://doi.org/10.1038/s41586-
520 020-2627-8.
521 Lenaerts, J. T. M., Vizcaino, M., Fyke, J., van Kampenhout, L., & van den Broeke, M. R. (2016). Present-day and future
522 Antarctic ice sheet climate and surface mass balance in the Community Earth System Model. Climate Dynamics, 47(5), 1367–
523 1381. https://doi.org/10.1007/s00382-015-2907-4
524 Lenaerts, J. T., Fyke, J., & Medley, B. (2018). The signature of ozone depletion in recent Antarctic precipitation change: A
525 study with the Community Earth System Model. Geophysical Research Letters, 45(23), 12-931.
526 https://doi.org/10.1029/2018GL078608
527 Li, S., Chen, Y., Wei, W., Fang, G., & Duan, W. (2024). The increase in extreme precipitation and its proportion over global
528 land. Journal of Hydrology, 628, 130456. https://doi.org/10.1016/j.jhydrol.2023.130456
529 Maclennan, M. L., Lenaerts, J. T., Shields, C., & Wille, J. D. (2022). Contribution of atmospheric rivers to Antarctic
530 precipitation. Geophysical Research Letters, 49(18), e2022GL100585. https://doi.org/10.1029/2022GL100585
531 Maclennan, M. L., Lenaerts, J., Shields, C. A., Hoffman, A. O., Wever, N., Thompson-Munson, M., ... & Wille, J. D. (2023).
532 Climatology and surface impacts of atmospheric rivers on West Antarctica. The Cryosphere, 17(2), 865-881.
533 https://doi.org/10.5194/tc-17-865-2023
534 Marshall, G. J. (2003). Trends in the Southern annular mode from observations and reanalyses. Journal of Climate, 16(24),
535 4134–4143. https://doi.org/10.1175/1520-0442(2003)016<4134:TITSAM>2.0.CO;2
536 Marshall, G. J., Orr, A., & Turner, J. (2013). A predominant reversal in the relationship between the SAM and East Antarctic
537 temperatures during the twenty-first century. Journal of Climate, 26(14), 5196-5204.
538 https://doi.org/10.1175/JCLI-D-12-00671.1
539 Meehl, G. A., Washington, W. M., Wigley, T. M. L., Arblaster, J. M., & Dai, A. (2003). Solar and greenhouse gas forcing and
540 climate response in the twentieth century. Journal of Climate, 16(3), 426-444.
541 https://doi.org/10.1175/1520-0442(2003)016<0426:SAGGFA>2.0.CO;2
542 Mémin, A., Flament, T., Alizier, B., Watson, C., & Rémy, F. (2015). Interannual variation of the Antarctic Ice Sheet from a
543 combined analysis of satellite gravimetry and altimetry data. Earth and Planetary Science Letters, 422, 150–156.
544 https://doi.org/https://doi.org/10.1016/j.epsl.2015.03.045
545 Min, S. K., Zhang, X., Zwiers, F. W., & Hegerl, G. C. (2011). Human contribution to more-intense precipitation extremes.
546 Nature, 470(7334), 378-381. https://www.nature.com/articles/nature09763

https://doi.org/10.5194/egusphere-2025-4292
Preprint. Discussion started: 23 September 2025

Morioka, Y., Zhang, L., Cooke, W., Nonaka, M., Behera, S. K., & Manabe, S. (2024). Role of anthropogenic forcing in Antarctic sea ice variability simulated in climate models. Nature Communications, 15(1), 10511. https://doi.org/10.1038/s41467-024-54485-7

Mottram, R., Hansen, N., Kittel, C., Van Wessem, J. M., Agosta, C., Amory, C., ... & Souverijns, N. (2021). What is the surface mass balance of Antarctica? An intercomparison of regional climate model estimates. The Cryosphere, 15(8), 3751-3784. https://doi.org/10.5194/tc-15-3751-2021

Munneke, P. K., Ligtenberg, S. R., Van Den Broeke, M. R., & Vaughan, D. G. (2014). Firn air depletion as a precursor of Antarctic ice-shelf collapse. Journal of Glaciology, 60(220), 205-214. https://doi.org/10.3189/2014JoG13J183

Nakayama, Y., Greene, C. A., Paolo, F. S., Mensah, V., Zhang, H., Kashiwase, H., ... & Aoki, S. (2021). Antarctic slope current modulates ocean heat intrusions towards Totten Glacier. Geophysical Research Letters, 48(17), e2021GL094149. https://doi.org/10.1029/2021GL094149

Nicola, L., Notz, D., & Winkelmann, R. (2023). Revisiting temperature sensitivity: how does Antarctic precipitation change with temperature?. *The Cryosphere*, *17*(7), 2563-2583. https://doi.org/10.5194/tc-17-2563-2023

Nicolas, J. P., and Coauthors, 2017: January 2016 extensive summer melt in West Antarctica favoured by strong El Niño. Nat. Commun., 8, 15799, https://doi.org/10.1038/ncomms15799.

Orr, A., Lu, H., Martineau, P., Gerber, E. P., Marshall, G. J., & Bracegirdle, T. J. (2021). Is our dynamical understanding of the circulation changes associated with the Antarctic ozone hole sensitive to the choice of reanalysis dataset?. *Atmospheric Chemistry and Physics*, *21*(10), 7451-7472. https://doi.org/10.5194/acp-21-7451-2021

Orr, A., Deb, P., Clem, K. R., Gilbert, E., Bromwich, D. H., Boberg, F., ... & Zou, X. (2023). Characteristics of surface "melt potential" over Antarctic ice shelves based on regional atmospheric model simulations of summer air temperature extremes from 1979/80 to 2018/19. Journal of Climate, 36(10), 3357-3383. https://doi.org/10.1175/JCLI-D-22-0386.1

Paik, S., Min, S. K., Zhang, X., Donat, M. G., King, A. D., & Sun, Q. (2020). Determining the anthropogenic greenhouse gas contribution to the observed intensification of extreme precipitation. Geophysical Research Letters, 47(12), e2019GL086875. https://doi.org/10.1029/2019GL086875

Paolo, F. S., Fricker, H. A., & Padman, L. (2015). Volume loss from Antarctic ice shelves is accelerating. Science, 348(6232), 327-331. DOI: 10.1126/science.aaa0940

Paolo, F., Padman, L., Fricker, H., Adusumilli, S., Howard, S., & Siegfried, M. (2018). Response of Pacific-sector Antarctic ice shelves to the el Niño/southern oscillation. Nature Geoscience, 11(2), 121–126. https://doi.org/10.1038/s41561-017-0033-0

Pattyn, F. (2017). Sea-level response to melting of Antarctic ice shelves on multi-centennial timescales with the fast Elementary Thermomechanical Ice Sheet model (f. ETISh v1. 0). The Cryosphere, 11(4), 1851-1878. https://doi.org/10.5194/tc-11-1851-2017

https://doi.org/10.5194/egusphere-2025-4292
Preprint. Discussion started: 23 September 2025

Pirani, S.L. Connors, C. Péan, S. Berger, N. Caud, Y. Chen, L. Goldfarb, M.I. Gomis, M. Huang, K. Leitzell, E. Lonnoy, J.B.R. Matthews, T.K. Maycock, T. Waterfield, O. Yelekçi, R. Yu, and B. Zhou (eds.)]. Cambridge University Press, Cambridge, United Kingdom and New York, NY, USA, pp. 1513–1766, doi: 10.1017/9781009157896.013.

Pope, J. O., Orr, A., Marshall, G. J., & Abraham, N. L. (2020). Non-additive response of the high-latitude Southern Hemisphere climate to aerosol forcing in a climate model with interactive chemistry. Atmospheric Science Letters, 21(12), e1004. https://doi.org/10.1002/asl.1004

Previdi, M., & Polvani, L. M. (2016). Anthropogenic impact on Antarctic surface mass balance, currently masked by natural variability, to emerge by mid-century. Environmental Research Letters, 11(9), 094001. DOI 10.1088/1748-9326/11/9/094001

Pritchard, H. D., S. R. M. Ligtenberg, H. A. Fricker, D. G. Vaughan, M. R. van den Broeke, and L. Padman, 2012: Antarctic ice-sheet loss driven by basal melting of ice shelves. Nature, 484, 502–505, https://doi.org/10.1038/nature10968.

Pritchard, H. D. (2021), Global data gaps in our knowledge of the terrestrial cryosphere, Front. Clim., 3, https://doi.org/10.3389/fclim.2021.689823

Ribes, A., Planton, S., & Terray, L. (2013). Application of regularised optimal fingerprinting to attribution. Part I: Method, properties and idealised analysis. Climate dynamics, 41, 2817-283 https://doi.org/10.1007/s00382-013-1735-7

Rignot, E., Mouginot, J., Scheuchl, B., van den Broeke, M., van Wessem, M. J., & Morlighem, M. (2019). Four decades of Antarctic ice sheet mass balance from 1979–2017. Proceedings of the National Academy of Sciences - PNAS, 116(4), 1095–1103. https://doi.org/10.1073/pnas.1812883116

Rott, H., P. Skvarca, and T. Nagler, 1996: Rapid collapse of northern Larsen Ice Shelf, Antarctica. Science, 271, 788–792, https://doi.org/10.1126/science.271.5250.788.

Scambos, T. A., C. Hulbe, M. Fahnestock, and J. Bohlander, 2000: The link between climate warming and break-up of ice shelves in the Antarctic Peninsula. J. Glaciol., 46, 516–530, https://doi.org/10.3189/172756500781833043.

Seneviratne, S.I., X. Zhang, M. Adnan, W. Badi, C. Dereczynski, A. Di Luca, S. Ghosh, I. Iskandar, J. Kossin, S. Lewis, F. Otto, I. Pinto, M. Satoh, S.M. Vicente-Serrano, M. Wehner, and B. Zhou, 2021: Weather and Climate Extreme Events in a Changing Climate. In Climate Change 2021: The Physical Science Basis. Contribution of Working Group I to the Sixth Assessment Report of the Intergovernmental Panel on Climate Change[Masson-Delmotte, V., P. Zhai, A.

Stenni, B., Curran, M. A., Abram, N. J., Orsi, A., Goursaud, S., Masson-Delmotte, V., ... & Frezzotti, M. (2017). Antarctic climate variability on regional and continental scales over the last 2000 years. Climate of the Past, 13(11), 1609-1634. https://doi.org/10.5194/cp-13-1609-2017

Shepherd, A., Ivins, E., Rignot, E., Smith, B., van den Broeke, M. R., Velicogna, I., Whitehouse, P., Briggs, K., Joughin, I., Krinner, G., Nowicki, S., Payne, T., Scambos, T. A., Schlegel, N., A, G., Agosta, C., Ahlstrøm, A., Babonis, G., Barletta, V., Blazquez, A., Bonin, J., Csatho, B., Cullather, R., Felikson, D., Fettweis, X., Forsberg, R., Gallée, H., Gardner, A., Gilbert, L., Groh, A., Gunter, B., Hanna, E., Harig, C., Helm, V., Horvath, A., Horwath, M., Khan, S., Kjeldsen, K. K., Konrad, H., Langen, P., Lecavalier, B., Loomis, B., Luthcke, S., McMillan, M., Melini, D., Mernild, S., Mohajerani, Y., Moore, P., Mouginot, J., Moyano, G., Muir, A., Nagler, T., Nield, G., Nilsson, J., Noël, B., Otosaka, I., Pattle, M. E., Peltier, W. R., Pie,

N., Rietbroek, R., Rott, H., Sandberg-Sørensen, L., Sasgen, I., Save, H., Scheuchl, B., Schrama, E., Schröder, L., Seo, K.-W., Simonsen, S., Slater, T., Spada, G., Sutterley, T., Talpe, M., Tarasov, L., van de Berg, W. J., van der Wal, W., van Wessem, M., Vishwakarma, B. D., Wiese, D., Wouters, B., and team, T. I.: Mass balance of the Antarctic Ice Sheet from 1992 to 2017, Nature, 558, 219–222, https://doi.org/10.1038/s41586-018-0179-y

Smith, K. L., & Polvani, L. M. (2017). Spatial patterns of recent Antarctic surface temperature trends and the importance of natural variability: lessons from multiple reconstructions and the cmip5 models. Climate Dynamics, 48(7), 2653-2670. DOI: 10.1007/s00382-016-3230-4

Simon, S., Turner, J., Thamban, M., Wille, J. D., & Deb, P. (2024). Spatiotemporal variability of extreme precipitation events and associated atmospheric processes over Dronning Maud Land, East Antarctica. Journal of Geophysical Research: Atmospheres, 129(7), e2023JD038993. https://doi.org/10.1029/2023JD038993

Simpson, I. R., Rosenbloom, N., Danabasoglu, G., Deser, C., Yeager, S. G., McCluskey, C. S., ... & Rodgers, K. B. (2023). The CESM2 single-forcing large ensemble and comparison to CESM1: Implications for experimental design. Journal of Climate, 36(17), 5687-5711. https://doi.org/10.1175/JCLI-D-22-0666.1

Stenni, B., Curran, M. A., Abram, N. J., Orsi, A., Goursaud, S., Masson-Delmotte, V., ... & Frezzotti, M. (2017). Antarctic climate variability on regional and continental scales over the last 2000 years. Climate of the Past, 13(11), 1609-1634. https://doi.org/10.5194/cp-13-1609-2017

Sun, Q., Zhang, X., Zwiers, F., Westra, S., & Alexander, L. V. (2021). A global, continental, and regional analysis of changes in extreme precipitation. Journal of Climate, 34(1), 243-258. https://doi.org/10.1175/JCLI-D-19-0892.1

Swart, N. C., Gille, S. T., Fyfe, J. C., & Gillett, N. P. (2018). Recent Southern Ocean warming and freshening driven by greenhouse gas emissions and ozone depletion. Nature Geoscience, 11(11), 836-841. https://doi.org/10.1038/s41561-018-0226-1

Swetha Chittella, S. P., Deb, P., & Melchior van Wessem, J. (2022). Relative contribution of atmospheric drivers to “extreme” snowfall over the Amundsen Sea Embayment. Geophysical Research Letters, 49(16), e2022GL098661. https://doi.org/10.1029/2022GL098661

The Community Earth System Model Version 2 (CESM2), G. Danabasoglu et al., 2020, https://doi.org/10.1029/2022GL098661

Thompson, D. W., & Solomon, S. (2002). Interpretation of recent Southern Hemisphere climate change. Science, 296(5569), 895-899. DOI: 10.1126/science.1069270

Trusel, L. D., K. E. Frey, S. B. Das, P. Kuipers Munneke, and M. R. van den Broeke, 2013: Satellite-based estimates of Antarctic surface meltwater fluxes. Geophys. Res. Lett., 40, 6148–6153, https://doi.org/10.1002/2013GL058138.

Turner, J., Phillips, T., Thamban, M., Rahaman, W., Marshall, G. J., Wille, J. D., ... & Lachlan-Cope, T. (2019). The dominant role of extreme precipitation events in Antarctic snowfall variability. Geophysical Research Letters, 46(6), 3502-3511. https://doi.org/10.1029/2018gl081517

https://doi.org/10.5194/egusphere-2025-4292
Preprint. Discussion started: 23 September 2025

van Wessem, J. M., van den Broeke, M. R., Wouters, B., & Lhermitte, S. (2023). Variable temperature thresholds of melt pond formation on Antarctic ice shelves. Nature Climate Change, 13(2), 161-166. https://doi.org/10.1038/s41558-022-01577-1

Vignon, É., Roussel, M. L., Gorodetskaya, I. V., Genthon, C., & Berne, A. (2021). Present and future of rainfall in Antarctica. Geophysical Research Letters, 48(8), e2020GL092281. https://doi.org/10.1029/2020GL092281

Wang, S., Alexander, P. M., Alley, R. B., Huang, Z., Parizek, B. R., Willet, A. G., & Anandakrishnan, S. (2025). Recent variability in fracture characteristics and ice flow of Thwaites Ice Shelf, West Antarctica. *Journal of Geophysical Research: Earth Surface*, *130*(5), e2024JF008118. https://doi.org/10.1029/2024JF008118

Wille, J. D., Favier, V., Gorodetskaya, I. V., Agosta, C., Kittel, C., Beeman, J. C., ... & Codron, F. (2021). Antarctic atmospheric river climatology and precipitation impacts. Journal of Geophysical Research: Atmospheres, 126(8), e2020JD033788. https://doi.org/10.1029/2020JD033788

Wille, J. D., Favier, V., Gorodetskaya, I. V., Agosta, C., Kittel, C., Beeman, J. C., ... & Codron, F. (2021). Antarctic atmospheric river climatology and precipitation impacts. Journal of Geophysical Research: Atmospheres, 126(8), e2020JD033788. https://doi.org/10.1029/2020JD033788

Wille, J. D., Favier, V., Jourdain, N. C., Kittel, C., Turton, J. V., Agosta, C., ... & Berchet, A. (2022). Intense atmospheric rivers can weaken ice shelf stability at the Antarctic Peninsula. Communications Earth & Environment, 3(1), 90. https://doi.org/10.1038/s43247-022-00422-9

Wille, J. D., Alexander, S. P., Amory, C., Baiman, R., Barthélemy, L., Bergstrom, D. M., ... & Zou, X. (2024a). The extraordinary March 2022 East Antarctica "heat" wave. Part II: Impacts on the Antarctic ice sheet. Journal of Climate, 37(3), 779-799. https://doi.org/10.1175/JCLI-D-23-0176.1

Wille, J. D., Alexander, S. P., Amory, C., Baiman, R., Barthélemy, L., Bergstrom, D. M., ... & Zou, X. (2024b). The extraordinary March 2022 East Antarctica "heat" wave. Part I: Observations and meteorological drivers. Journal of Climate, 37(3), 757-778. https://doi.org/10.1175/JCLI-D-23-0175.1

Wille, J. D., Favier, V., Gorodetskaya, I. V., Agosta, C., Baiman, R., Barrett, J. E., ... & Zhang, Z. (2025). Atmospheric rivers in Antarctica. Nature Reviews Earth & Environment, 6(3), 178-192. https://doi.org/10.1038/s43017-024-00638-7

Yu, L., Yang, Q., Vihma, T., Jagovkina, S., Liu, J., Sun, Q., & Li, Y. (2018). Features of extreme precipitation at Progress Station, Antarctica. Journal of Climate, 31(22), 9087-9105. https://doi.org/10.1175/JCLI-D-18-0128.1

Yu, L., Zhong, S., Jagovkina, S., Sui, C., & Sun, B. (2025). Interannual Variability and Trends in Extreme Precipitation in Dronning Maud Land, East Antarctica. Remote Sensing, 17(2), 324. https://doi.org/10.3390/rs17020324

Zhang, B., Yao, Y., Liu, L. & Yang, Y. Interannual ice mass variations over the Antarctic ice sheet from 2003 to 2017 were linked to El Niño-Southern oscillation. Earth Planet. Sci. Lett. 560, 116796 (2021). 10.1016/j.epsl.2021.116796 DOI: 10.1016/j.epsl.2021.116796

Zhu, Z., Liu, J., Song, M., & Hu, Y. (2023). Changes in extreme temperature and precipitation over the southern extratropical continents in response to Antarctic Sea ice loss. Journal of Climate, 36(14), 4755-4775. https://doi.org/10.1175/JCLI-D-22-0577.1

https://doi.org/10.5194/egusphere-2025-4292
Preprint. Discussion started: 23 September 2025

680 Zwally, H. J., Robbins, J. W., & Luthcke, S. B. (2017). Mass balance of east Antarctic ice sheet: Reconciling icesat altimetry
681 with grace gravimetry and long-term ice history. In Agu fall meeting abstracts (Vol. 2017, p. C23D–08). DOI:
682 https://doi.org/10.1017/jog.2021.8